

Waves in Plasmas (Pergamon, New York, 1970), Sect. 20; J. P. Friedberg, R. W. Mitchell, R. L. Morse, and L. I. Rudsinski, Phys. Rev. Lett. **28**, 795 (1972).

⁶Megagauss magnetic fields were first identified as due to resonance absorption in computer simulations by A. B. Langdon and B. F. Lasinski (private communication). D. W. Forslund and E. L. Lindman have also observed dc magnetic fields in simulations (private communication).

⁷J. A. Stamper and D. A. Tidman, Phys. Fluids **16**, 2024 (1973).

⁸L. D. Landau and E. M. Lifshitz, *Electrodynamics of Continuous Media* (Pergamon, New York, 1960), p. 256; L. P. Pitaevskii, Zh. Eksp. Teor. Fiz. **39**, 1450

(1960) [Sov. Phys. JETP **12**, 1008 (1961)].

⁹N. A. Krall and A. W. Trivelpiece, *Principles of Plasma Physics* (McGraw-Hill, New York, 1973), pp. 315-317.

¹⁰A. B. Langdon and B. F. Lasinski, in "Methods in Computational Physics," edited by J. Killeen *et al.* (Academic, New York, to be published), Vol. 16.

¹¹K. G. Estabrook, E. J. Valeo, and W. L. Kruer, "Two-Dimensional Relativistic Simulations of Resonance Absorption" (to be published), Figs. 2 and 3.

¹²K. G. Estabrook, E. J. Valeo, and W. L. Kruer, Phys. Lett. **49A**, 109 (1974).

¹³E. J. Valeo and K. G. Estabrook, Phys. Rev. Lett. **34**, 1008 (1975).

Electromagnetic Ion-Beam Instabilities in the Solar Wind*

Michael D. Montgomery, S. Peter Gary, D. W. Forslund, and W. C. Feldman
Los Alamos Scientific Laboratory, University of California, Los Alamos, New Mexico 87544

(Received 14 May 1975)

The stability of a plasma consisting of two, unequal, isotropic, ion beams streaming along a uniform magnetic field has been investigated by numerically solving the full electromagnetic, Vlasov, linear dispersion relation for high- β plasmas. Three instabilities are found: One is closely associated with the usual Alfvén mode and the two others with the "fast" or magnetosonic mode. The importance of these instabilities for certain neutral-beam-injection experiments and in the solar wind is emphasized.

Recent IMP-6 solar-wind observations^{1,2} have shown the regular appearance of persistent, double-peaked, ion-velocity distributions. The two peaks are generally unequal in size, are often clearly resolved, and may be separated by as much as the local Alfvén speed C_A parallel to the ambient magnetic field \vec{B}_0 . Since $\beta = 8\pi nT/B_0^2$ is moderately high, it is appropriate to utilize the complete electromagnetic dispersion relation. For this study the range $0.05 \leq \beta \leq 1$ is considered. This range is also of interest for future neutral-beam-heating experiments in moderately dense plasmas.³

Theoretical investigation of electromagnetic ion-beam instabilities effectively began with Stepanov and Kitsenko.⁴ They concluded that both right- and left-hand circularly polarized modes (commonly termed magnetosonic and Alfvén waves, respectively) propagating parallel to \vec{B}_0 could be driven unstable by a weak, secondary ion beam also directed along \vec{B}_0 . However, these results are subject to question because they calculated growth rates from frequencies which did not include either the particle thermal velocities or contributions due to the beam. Later work^{5,6} has used the same questionable technique.

More recently, growth rates for ion-beam ve-

locities much greater than the Alfvén speed C_A have been calculated,⁷ and the special case of propagation perpendicular to the ambient magnetic field for equal-density components has been treated.⁸ Growth rates for obliquely propagating electrostatic ion-cyclotron waves in a warm plasma have also been evaluated.⁹

This Letter presents selected results from a more general investigation of electromagnetic ion-beam instabilities carried out by numerically solving the electromagnetic, Vlasov, linear dispersion relation for a homogeneous plasma including off-angle propagation.¹⁰ These results represent substantial improvements over those obtained with use of the cold-plasma approximation.

For this study, a three-component plasma configuration is assumed, consisting of a main proton component (hereafter denoted by the subscript M), a counterstreaming (in the center-of-mass frame), secondary proton component (beam) denoted by the subscript B , and an electron component e , where each component is assumed to be an isotropic Maxwellian. The plasma is electrically neutral, $n_M + n_B = n_e$, and bears no current, $n_M V_{0M} + n_B V_{0B} = 0$ and $V_{0e} = 0$. The V_{0j} are the drift velocities of the various ($j = M, B, e$)

components relative to the center of mass of the entire system. Temperature anisotropies have been ignored, even though they can be substantial in the solar wind, in order to isolate the effects of the counterstreaming, unequal beams.

We now discuss numerical results for one representative case typical of the solar wind as well as high- β plasmas of current interest. The configuration is defined as follows: $T_B = T_M$, $T_e/T_M = 2$, $n_B/n_M = 0.3$, $C_A^2/c^2 = B_0^2/4\pi m_p n_e c^2 = 4.8 \times 10^{-8}$, where $V_D = |V_{0B} - V_{0M}|$ and $\beta_M = 8\pi n_e T_M/B_0^2$ are variable. For zero drift ($V_D = 0$) and $ka_p < 1$ [the proton thermal Larmor radius is $a_p = V_p/\Omega_p = (T_p/m_p)^{1/2}/(eB_0/m_p c)$], the numerical solutions of real frequency as a function of wave number $\omega(\vec{k})$ correspond to the three well-known ("fast," "intermediate," and "slow") modes of low- β magnetohydrodynamic (MHD) theory.¹¹ A study of the stability of this configuration for $V_D \neq 0$ as a function of β_M shows that, depending on β_M , three different instabilities can become important. The slow mode was found to be damped and will not be further considered. The three unstable modes are clearly recognizable in Fig. 1 as three distinct threshold curves labeled A, B,

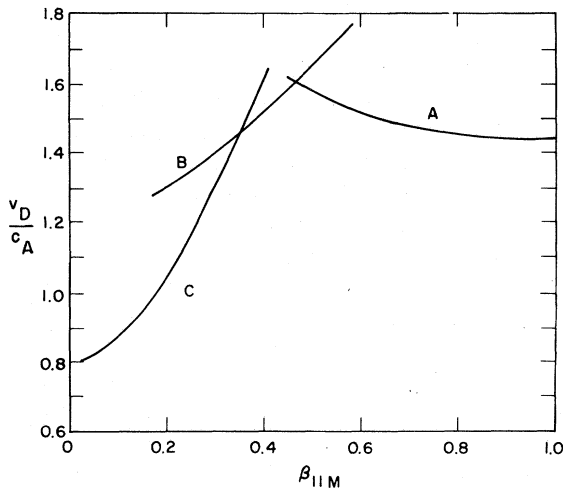


FIG. 1. Drift-velocity thresholds as a function of parallel β for the main proton component ($\beta_{\parallel M} = 8\pi n_e T_{\parallel M}/B_0^2$). In this case $\beta_{\parallel M} = \beta_M$ because $T_{\parallel M} = T_M$. The threshold is arbitrarily defined as $\lambda/\Omega_p = 10^{-4}$ —a growth rate high enough to become important in the solar wind where $\Omega_p \sim 0.5 \text{ sec}^{-1}$ and the characteristic expansion time is $\approx 10^5 \text{ sec}$, as well as in laboratory experiments where $\Omega_p \sim 10^8 \text{ sec}^{-1}$ and confinement times are $\sim 10^{-3} \text{ sec}$. The dispersive properties and polarization of the three modes labeled A, B, and C (summarized in Table I) make it clear that modes A and B are associated with the magnetosonic mode while mode C is predominantly an Alfvén mode.

and C. Brief inspection of the polarization and dispersive properties of these modes (summarized in Table I) makes it clear that modes A and B are associated with the so-called MHD mode and will be termed here field-aligned and oblique magnetosonic modes, respectively. Mode C is the intermediate MHD or Alfvén mode and will be referred to as the ion-beam Alfvén instability.

The major characteristics of the various modes can be summarized as follows: The field-aligned magnetosonic mode (mode A) is characterized by a steeply (then more slowly) rising growth rate with increasing V_D , increasing to $\gamma/\Omega_p \geq 0.2$ for $V_D/C_A \sim 2$ with ka_p at maximum growth rate γ_{max} remaining about constant at ~ 0.3 . This mode is purely electromagnetic and right-hand circularly polarized. Near threshold it is only unstable when \vec{k} is very nearly parallel to \vec{B}_0 (i.e., \vec{k} must lie inside of a cone of a few degrees half angle when $\gamma/\Omega_p \sim 10^{-4}$), but at larger growth rates the cone half angle for $\frac{1}{2}$ the maximum growth rate increases to several tens of degrees. For example when V_D/C_A exceeds 20 (where $\gamma/\Omega_p \sim 0.5$) the half angle becomes 75° . The growth rates do not go through a maximum with respect to V_D , but continue to increase slowly out to a V_D/C_A of at least 25. For $\beta_M \leq 0.3$, the threshold of the field-aligned instability rises significantly above that of the other modes (Fig. 1).

At intermediate β_M the oblique ion-beam magnetosonic mode (mode B) has the lowest threshold and is characterized by the following properties: γ rises steeply with V_D above threshold but tends to saturate at values about a factor of 10 below that for the field-aligned case. For example, at

TABLE I. Wave characteristics at threshold.

Type, β	Polarization ^a	ka_p	$u = \cos\theta$	$\frac{\omega/k}{C_A}$	$\frac{\delta E}{\delta B}$ ^b	$\frac{\delta E_{\parallel}}{\delta E_{\perp}}$ ^c
A, 1.0	1.0	0.3	1.0	1.13	1.0	0.0
A, 0.5	1.0	0.27	1.0	1.16	1.0	0.0
B, 0.5	0.56	0.1	0.92	1.0	1.07	0.5
B, 0.2	0.5	0.02	0.96	0.94	1.02	0.3
C, 0.3	-8.3	0.13	0.77	0.6	1.55	0.75
C, 0.05	-1.15	0.12	0.94	0.6	1.06	0.32

^a1.0 for circular polarization; 0 or ∞ for linear polarization; negative value for left-hand polarization.

^bRatio of electric to magnetic fluctuation amplitudes (normalized so that $\delta E/\delta B = 1$ for a pure electromagnetic mode).

^cRatio of parallel to perpendicular (to \vec{k}) electric field fluctuation amplitudes.

$V_D/C_A = 2$ and $\beta_M = 0.3$, $\gamma_{\max}/\Omega_p \sim 0.02$. It appears that at very high drifts ($V_D/C_A \gtrsim 10$) the growth rates saturate and the field-aligned mode *A* (even at $\beta_M \leq 0.2$) dominates. Near threshold, the oblique mode is composed of mixed transverse and longitudinal components although predominantly electromagnetic, and is right-hand elliptically polarized. ka_p ranges from 0.02 to 0.1 near threshold with $\omega/k \approx C_A$.

At still lower β_M , the Alfvén mode has the lowest threshold, but on the other hand is the weakest of the three instabilities. γ becomes maximum near $(2-3) \times 10^{-2} \Omega_p$ for $V_D/C_A \approx 1$ and decreases slowly for $V_D/C_A > 1$. As in the case of the oblique magnetosonic mode, the beam Alfvén mode is stable and moderately damped for $\vec{k} \parallel \vec{B}_0$. Phase speeds relative to the center-of-mass frame are normally significantly below the Alfvén speed.

In order to identify the physical processes that are important with respect to the fastest growing of these instabilities, the field-aligned magnetosonic mode, we have found it useful to compare solutions of the much more tractable cold-plasma dispersion relation with numerical calculations similar to those already described. In this case, however, we need only consider $\vec{k} \parallel \vec{B}_0$, and the dispersion relation is much simpler.¹²

For the following discussion, the same plasma configuration as already described was employed except for the minor changes noted in the caption to Fig. 2. The results of the comparison are illustrated in Fig. 2 and can be summarized as follows: (1) For $ka_p \ll 1$ and for $V_{0B} \gg C_A$, the cold-plasma dispersion relation (with drift velocities and beam contributions included) gives a good approximation to the Vlasov results for both ω and γ . When either of the above inequalities is satisfied, the $\vec{k} \parallel \vec{B}_0$ ion-beam instability can be clearly identified as a nonresonant fluid instability. (2) Near threshold ($V_{0B} \sim C_A$) and at shorter wavelengths ($ka_p \lesssim 1$) where the maximum growth rates are found, the cold-plasma approximation of γ becomes quite poor (in the direction of excessive stability). This is because an increasing number of particles in the beam component become cyclotron resonant and the threshold drift velocity is substantially lowered.

Thus, an important result of comparison with cold-plasma theory is that finite-Larmor-radius effects tend to destabilize significantly what at longer wavelengths is an ion-beam fluid instability. This is an additional example of a similar effect already found in the case of the well-

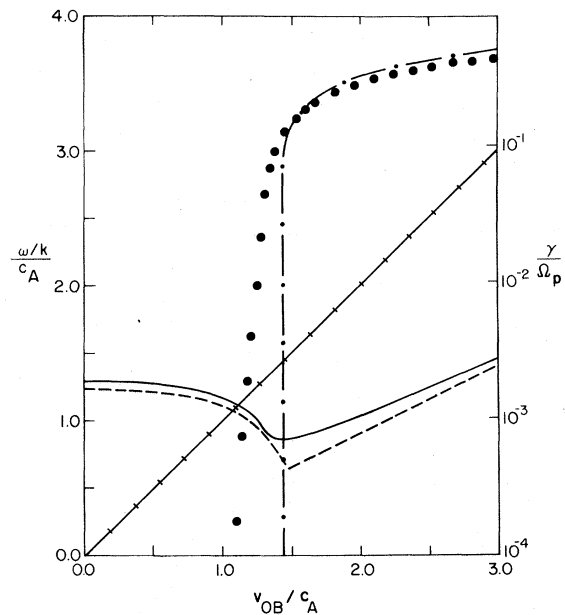


FIG. 2. Comparison of phase speeds and growth rates between Vlasov and cold-plasma theory as a function of proton-beam drift velocity V_{0B} (for V_{0B} and \vec{k} parallel to \vec{B}_0). The Vlasov (cold) plasma values for ω/k are shown by the solid (dashed) lines while γ is indicated by the dotted (dot-dashed) lines. For purposes of comparison $\omega/k = V_{0B}$ is indicated by the straight, hatched line. The plasma configuration is the same as for Fig. 1 except that β_M is fixed at 1.0, $C_A^2/c^2 = 2.0 \times 10^{-8}$, and $n_B/n_M = 0.43$ instead of 0.3. These changes make no qualitative difference in the results. $ka_p = 0.3$ for the Vlasov case.

known firehose instability.¹³ Such destabilization effects may be a general property of resonant ions with regard to electromagnetic instabilities.

Finally, although all of the instabilities considered here are likely to be important in the solar wind as well as other astrophysical plasmas, the field-aligned magnetosonic mode may also be particularly important in the case of laboratory fusion plasmas heated by neutral-particle injection parallel to \vec{B}_0 (for relatively high $\beta > 0.05$). In this case, at least for a time after beam switch-on and probably even under conditions of steady-state injection, a more or less well-defined secondary beam is expected to form.¹⁴ Since for $V_D \gg C_A$ and $n_B/n_M \sim 0.3$ the linear growth rates become very large ($0.5\Omega_p$) over a large volume of k space, the characteristic time for energy randomization due to the instability may be significantly shorter than the "deceleration time" for the ions due to collisions.¹⁵ A similar situation for the case of cross-field in-

jection has been found as a result of the electromagnetic cyclotron instability driven by $T_{i\perp} > T_{i\parallel}$.¹⁶

The analysis may also explain why apparently no anomalous beam diffusion has been observed to date in parallel-injection experiments. Figure 1 shows that ion-beam instabilities require injection velocities $V_D \sim C_A$, but recent experiments conducted at low $\beta \lesssim 0.005$ have used $V_D \sim 10V_p \lesssim C_A/4$. Instability thus requires a toroidal ion β of about 0.05, far in excess of the presently attainable values in tokamaks.

*Work performed under the auspices of the U. S. Energy Research and Development Administration.

¹W. C. Feldman, J. R. Asbridge, S. J. Bame, and M. D. Montgomery, *J. Geophys. Res.* **78**, 2017 (1973).

²W. C. Feldman, J. R. Asbridge, S. J. Bame, and M. D. Montgomery, *Rev. Geophys. Space Phys.* **12**, 715 (1974).

³H. L. Berk *et al.*, in *Proceedings of the Fifth International Conference on Plasma Physics and Controlled Nuclear Fusion Research, Tokyo, Japan, 1974* (International Atomic Energy Agency, Vienna, Austria, 1975), Paper No. G2-3.

⁴K. N. Stepanov and A. B. Kitsenko, *Zh. Tekh. Fiz.* **31**, 107 (1961) [*Sov. Phys. Tech. Phys.* **6**, 120 (1961)].

⁵J. Rowlands, V. D. Shapiro, and V. I. Shevchenko, *Zh. Eksp. Teor. Fiz.* **50**, 979 (1966) [*Sov. Phys. JETP* **23**, 651 (1966)].

⁶J. Prienhaelter and J. Václavik, *Plasma Phys.* **9**, 653 (1967).

⁷A. Barnes, *Cosmic Electroduct.* **1**, 90 (1970).

⁸J. D. Gaffey, W. B. Thompson, and C. S. Liu, *J. Plasma Phys.* **9**, 17 (1973).

⁹F. S. Weibel, *Phys. Fluids* **13**, 3003 (1970).

¹⁰T. H. Stix, *The Theory of Plasma Waves* (McGraw-Hill, New York, 1962), Chaps. 8 and 9.

¹¹See, for example, S. P. Gary, W. C. Feldman, D. W. Forslund, and M. D. Montgomery, "Heat-Flux Instabilities in the Solar Wind" (to be published).

¹²J. M. Cornwall and M. Schulz, *J. Geophys. Res.* **76**, 1191 (1971), and **78**, 6830(E) (1973).

¹³D. W. Forslund, in *Proceedings of the Solar Wind Conference, Asilomar, California, 1971*, edited by C. P. Sonett, J. M. Wilcox, and P. J. Coleman, Jr., NASA Special Publication No. 308 (U. S. National Aeronautics and Space Administration, Washington, D. C., 1972), p. 346; W. Pilipp and H. J. Völk, *J. Plasma Phys.* **6**, 1 (1971).

¹⁴T. H. Stix, *Phys. Fluids* **16**, 1922 (1973).

¹⁵Berk *et al.*, Ref. 3; F. W. Perkins, "Ion Streaming Instabilities: Electromagnetic and Electrostatic" (to be published).

¹⁶R. C. Davidson and J. M. Ogden, "Electromagnetic Ion Cyclotron Instability Driven by Ion Energy Anisotropy in High-Beta Plasmas" (to be published).

Two-Phonon Spectrum of Diamond*†

Riccardo Tubino‡ and Joseph L. Birman

Physics Department, City College of the City University of New York, New York, New York 10031

(Received 23 June 1975)

A careful calculation of the one-phonon dispersion in diamond reveals a shallow maximum in the [100] direction for the Δ_2' (LO) branch. The two-phonon (overtone) density of states shows a sharp peak near twice the Raman frequency. This supports the interpretation of an observed peak in two-phonon Raman scattering as a simple overtone without the need to invoke a two-phonon bound state.

The recent careful experimental investigation of the Raman spectrum of diamond¹ has stimulated considerable theoretical work attempting to explain the observed spectral features. Particular attention has been given to the origin of the sharp, polarized peak in the Stokes Raman scattering at an energy shift slightly above twice the one-phonon zone-center phonon energy and with symmetry $\Gamma^{(1+)}$. It has been proposed that this peak represents a two-phonon bound state.² In the present work we present new theoretical results which give strong support to interpreting this feature as an ordinary two-phonon overtone, arising from novel phonon dispersion in diamond.

The essential point of our work has been a very careful investigation of the phonon dispersion in diamond using a fine grid for calculating $\omega(\vec{q})$. We used a valence-force-field model³ which gives excellent agreement with the $\omega(\vec{q})$ determined from inelastic neutron scattering. The same model was also successful (with different parameters) in investigating phonon dispersion in silicon and germanium.³ In Fig. 1 we show phonon dispersion in diamond in the direction $\vec{q} \parallel \Delta[100]$. The calculated points are shown. To be noted is the shallow maximum in the branch $\Delta_2'(0)$ at q approximately $\frac{1}{3}$ of the zone boundary (X point). This maximum in this branch is approximately